

## Oligopeptidase B from *Trypanosoma evansi*

A PARASITE PEPTIDASE THAT INACTIVATES ATRIAL NATRIURETIC FACTOR IN THE BLOODSTREAM OF INFECTED HOSTS\*

Received for publication, September 1, 2004, and in revised form, January 10, 2005  
Published, JBC Papers in Press, January 11, 2005, DOI 10.1074/jbc.M410066200

Rory E. Morty<sup>‡§</sup>, Roger Pellé<sup>¶</sup>, István Vadász<sup>‡</sup>, Graciela L. Uzcanga<sup>||\*\*</sup>, Werner Seeger<sup>‡</sup>,  
and José Bubis<sup>\*\*</sup>

From the <sup>‡</sup>Department of Internal Medicine, University of Giessen Medical Centre, Aulweg 123 (Raum 6-11), D-35392 Giessen, Germany, the <sup>¶</sup>International Livestock Research Institute, P. O. Box 30709, Nairobi, Kenya, and the <sup>\*\*</sup>Departamento de Biología Celular, Universidad Simón Bolívar, Apartado 89.000, Valle de Sartenejas, Caracas 1081-A, Venezuela

Serine oligopeptidases of trypanosomatids are emerging as important virulence factors and therapeutic targets in trypanosome infections. We report here the isolation and characterization of oligopeptidase B (OpdB) and its corresponding gene from *Trypanosoma evansi*, a pathogen of significant veterinary importance. The *T. evansi* *opdB* gene was present as a single copy per haploid genome containing an open reading frame of 2148 bp encoding a protein of 80.664 kDa. Purified OpdB hydrolyzed substrates with basic residues in P<sub>1</sub> ( $k_{cat}/K_m$  for carbobenzyloxy-L-arginyl-L-arginyl-7-amido-4-methylcoumarin,  $337\text{ s}^{-1}\cdot\mu\text{M}^{-1}$ ) and exhibited potent arginyl carboxypeptidase activity ( $k_{cat}/K_m$  for Val-Lys-Arg ↓ Arg-OH,  $231\text{ s}^{-1}\cdot\text{mM}^{-1}$ ). While not secreted, *T. evansi* released OpdB into the plasma of infected hosts where it retained catalytic activity. Plasma OpdB levels correlated with blood parasitemia. *In vitro*, OpdB cleaved the peptide hormone atrial natriuretic factor (ANF) at four sites: Arg<sup>3</sup> ↓ Arg<sup>4</sup>, Arg<sup>4</sup> ↓ Ser<sup>5</sup>, Arg<sup>11</sup> ↓ Ile<sup>12</sup>, and Arg<sup>27</sup> ↓ Tyr<sup>28</sup>, thereby abrogating smooth muscle relaxant and prohypotensive properties of ANF. Circulating plasma ANF levels in *T. evansi*-infected rats were depressed from 130 to 8 pg·ml<sup>-1</sup>, and plasma ANF levels inversely correlated with plasma OpdB activity. The *in vitro* half-life of ANF in rat plasma was reduced 300-fold in plasma from *T. evansi*-infected rodents, which contains high levels of OpdB activity. Addition of OpdB inhibitors to cell-free plasma from infected rodents significantly abrogated this ANF hydrolysis. Furthermore the *in vivo* ANF half-life was reduced 5-fold in *T. evansi*-infected rats. Thus, we propose a role for OpdB in peptide hormone dysregulation in trypanosomiasis, specifically in generating the depressed plasma levels of ANF in mammals infected with *T. evansi*.

\* This work was supported by grants from the Alexander von Humboldt Foundation (to R. E. M.), the Deutsche Forschungsgemeinschaft Sonderforschungsbereich 547: "Kardiopulmonales Gefäßsystem" (to R. E. M., I. V., and W. S.), and Fondo Nacional de Ciencia, Tecnología e Innovación Grant G-2000001152 (to J. B.). The costs of publication of this article were defrayed in part by the payment of page charges. This article must therefore be hereby marked "advertisement" in accordance with 18 U.S.C. Section 1734 solely to indicate this fact.

The nucleotide sequence(s) reported in this paper has been submitted to the GenBank™/EBI Data Bank with accession number(s) AY546084.

§ To whom correspondence should be addressed. Tel: 49-(641)-994-2303; Fax: 49-(641)-994-2308; E-mail: rory.morty@innere.med.uni-giessen.de.

|| Present address: Dept. de Sanidad Animal, Facultad de Veterinaria, Universidad Complutense de Madrid, Avenida Puerta de Hierro s/n, 28040 Madrid, Spain.

The protozoan parasite *Trypanosoma evansi* (Steele 1885) is the etiological agent of a disease called surra, which is a major cause of livestock morbidity and mortality (1) and is thus of significant economic importance in affected areas. It has the broadest geographic (1) and host (2) ranges of any pathogenic trypanosome. Acute infection causes a severe febrile illness characterized by coughing, dyspnea, pulmonary edema, idiopathic cardiomyopathy, hepatosplenomegaly and immunosuppression, and death by respiratory distress or cardiac failure (1).

The pathogenic mechanisms underlying the development of these lesions have not been elucidated, although they are often attributed to bioactive substances, such as peptidases, phospholipases, lipopolysaccharides, and free fatty acids, released into the host circulation by dead and dying parasites (3). Parasite-derived peptidases in particular are emerging as important pathogenic factors, and candidates include a cell surface metallopeptidase, gp63 (4), a cysteine peptidase (5), and a secreted collagenolytic serine peptidase (6). Other parasite peptidases enter the host circulation upon intravascular destruction of the parasites (7). These peptidases hydrolyze biologically significant substrates *in vitro*. For example, a trypanosome cysteine peptidase can generate Lys-bradykinin from kininogen and can activate pre-kallikrein (8). However, these peptidases are rapidly inhibited by host plasma peptidase inhibitors upon release into the bloodstream. gp63 is complexed by  $\alpha_2$ -macroglobulin (9), and trypanosome cysteine peptidases are rapidly ( $k_a \approx 5 \times 10^7\text{ M}^{-1}\cdot\text{s}^{-1}$ ) and tightly ( $K_i \approx 5\text{ }\mu\text{M}$ ) complexed with cystatins and kininogen (10, 11) with concomitant loss of catalytic activity. Thus, their catalytic activity in the host bloodstream is unlikely to contribute to pathology. Indeed no trypanosome cysteine peptidase activity is found in plasma from *Trypanosoma brucei*-infected rodents (10). In contrast, a small subset of parasite peptidases is not affected by plasma peptidase inhibitors, and these peptidases retain their catalytic activity in the host bloodstream. Two members of the prolyl oligopeptidase family exemplify this group of peptidases. Oligopeptidase B (OpdB)<sup>1</sup> has been identified in *T. brucei* (12) and *Trypanosoma congolense* (13), which cause African trypanosomiasis, and also in *Trypanosoma cruzi*, which causes Chagas disease (14). A second oligopeptidase,

<sup>1</sup> The abbreviations used are: OpdB, oligopeptidase B; AMC, 7-amino-4-methylcoumarin; Mes, 4-morpholineethanesulfonic acid; ANF, atrial natriuretic factor;  $\beta$ NA,  $\beta$ -naphthylamine; Cbz, *N*-carbobenzyloxy; CHN<sub>2</sub>, diazomethyl ketone; DCI, 3,4-dichloroisocoumarin; E-64, *L*-trans-epoxysuccinyl-L-leucylamido(4-guanidino)butane; HPLC, high performance liquid chromatography; LPS, lipopolysaccharide; MALDI-TOF, matrix-assisted laser desorption ionization time-of-flight; SBTI, soybean trypsin inhibitor; Tricine, *N*-[2-hydroxy-1,1-bis(hydroxymethyl)ethyl]glycine; m/v, mass/volume.

prolyl oligopeptidase (Tc80), has been characterized from *T. cruzi* (15, 16). The inability of the host to regulate the catalytic activity of these two peptidases is significant since in the bloodstream they are brought into contact with host peptide hormones. Abnormal degradation of these hormones could impair host physiological homeostasis, an idea supported by the reduction in plasma levels of some peptide hormones observed in trypanosome infections (17), the unusual cleavage observed when peptide hormones are incubated in serum from trypanosome-infected rodents (18), and reports of endocrine dysfunction after trypanosome lysis in the host bloodstream (19).

In this study, we isolated, characterized, and cloned the gene encoding OpdB from *T. evansi*, the first peptidase ever cloned and characterized from this important veterinary pathogen. We then used a rodent model of *T. evansi* infection to address the following question: can peptidases released intravascularly by trypanosomes modulate peptide hormone levels in hosts? Although reports exist that document the extracellular release of parasite peptidases, this phenomenon has never been linked to the abnormal peptide hormone metabolism observed in trypanosome-infected hosts. Our data indicate that trypanosome peptidases can modulate circulating host peptide hormone levels. This has significant implications for our understanding of the pathogenesis of trypanosomiasis in particular the dysregulation of processes controlled by peptide hormones that are perturbed in trypanosome infections. These include hypotension (20), elevated blood volume (21), and dysregulation of the renin-angiotensin system (17) and the hypothalamic-pituitary-adrenal (22) and pituitary-gonadal axes (23).

#### MATERIALS AND METHODS

**Parasites**—*T. evansi* TEVA1 was obtained from a horse naturally infected in the Venezuelan savannah (24), while *T. evansi* IL3298 was obtained from a naturally infected camel from Marsabit, Kenya (25). Both *T. brucei* ILTat 1.1 and *T. cruzi* Y strain were passaged and propagated as described previously (12, 14). Experimental animal protocols were approved by local and national authorities.

**Gel Electrophoresis and Western Blotting**—Tris-Tricine SDS-PAGE (26) and immunoblotting with anti-OpdB IgY was performed as described previously (13).

**Purification of OpdB from Parasite Lysates**—OpdB was isolated from *T. evansi* TEVA1 lysates exactly as described for *T. congolense* (13) except that the *para*-aminobenzamidine-Sepharose column was replaced with an agmatine-Sepharose column (200 × 15 mm, 1 ml·min<sup>-1</sup>), and bound protein was eluted with 150 mM NaCl in 50 mM Tris-Cl, 1 mM dithiothreitol, pH 8.

**Cloning, Sequencing, and Site-directed Mutagenesis of the opdB Gene**—*T. evansi* strain IL3298 genomic DNA was isolated as described previously (12). Forward (5'-GGT GGA AGA GAA GCT TAT CAC AGG G-3') and reverse (5'-CGT CTT GTC GAT GTT AGC CCC CAC AC-3') primers were synthesized to be complementary to non-coding sequences flanking the *T. brucei* *opdB* open reading frame (GenBank™ accession number AF078916 (12)). PCR products were cloned into pGEM-T-Easy (Invitrogen) to create pRM157. Gene copy number was determined by Southern blot probed with a [<sup>32</sup>P]dCTP-labeled *opdB* open reading frame from pRM157 as described previously (12). Protein and DNA sequences were compared with ClustalW software from the MEGALIGN program (DNASTAR, Madison, WI) with a PAM250 weight table set with the following parameters: ktuple = 1, gap penalty = 3, and gap window = 5 (27).

**Hyperexpression of Recombinant OpdB**—The *T. evansi* IL3298 *opdB* gene was amplified by PCR from pRM157 with *Pfu* Turbo polymerase (Stratagene) using forward (5'-GG ACA **CAT ATG ATG** CAA ACT GAA CGT GGT CC-3') and reverse (5'-TAC GCT **CAT ATG** CTA CTT CCG CAG CAG CGG CC-3') primers (with internal NdeI sites in bold type; the initiation codon of the forward primer is underlined). The blunt-ended PCR product was cloned into the SmaI site of pBlueScript II KS(+) to create pRM158, and the 2.2-kb NdeI-NdeI fragment was excised from pRM158 and subcloned into the pET19b expression vector (Novagen) to create pRM159. The OpdB active site serine was converted to an alanine residue by site-directed mutagenesis using the QuikChange™ system (Stratagene) with forward (5'-TGC GAG GGA AGA **GCT** GCT GGT GGA TTG-3') and reverse (5'-CAA TCC ACC AGC

**AGC** TCT TCC CTC GCA-3') primers (the mutated codon is underlined, and the base pair changes are in bold type) and pRM159 as template, creating pRM160. Plasmids were transformed into *Escherichia coli* BL21(ADE3), and N-terminal polyhistidine-tagged fusion proteins were expressed as described previously (28).

**Immunoaffinity Purification of anti-OpdB IgY**—Recombinant OpdB (30 mg) was coupled to cyanogen bromide-activated Sepharose 4B (30 ml, packed volume) (29). Coupling efficiency was estimated at 92%. Anti-OpdB IgY (100 mg) was affinity-purified on an OpdB-Sepharose affinity chromatography column as described previously (13) with an estimated affinity-purified antibody yield of 9%. Affinity-purified antibodies were dialyzed extensively against Ringer's solution (4 × 6 h, 4 °C) to remove residual reagents left over from the affinity purification procedure. Antibody preparations were concentrated in Centricon™ concentrators (30-kDa cut-off, Millipore) according to the manufacturer's instructions.

**Enzymatic Characterization of OpdB**—Activity of OpdB was routinely determined against 5 μM *N*-carbobenzyloxy (Cbz)-L-Arg-L-Arg-7-amido-4-methylcoumarin (AMC) at 37 °C in 50 mM Tris-Cl, 5 mM dithiothreitol, pH 8.0 in a Hitachi F-2000 spectrofluorometer (λ<sub>ex</sub> = 370 nm, λ<sub>em</sub> = 460 nm) (12). Protein assays were conducted according to Bradford (30). Active enzyme concentration was determined with 4-methylumbelliferyl-*p*-guanidinobenzoate (12). Substrate specificity of native and recombinant *T. evansi* OpdB was determined using AMC- or β-naphthylamine (βNA)-derived fluorogenic peptide substrates (Bachem) as described previously (12). For carboxypeptidase activity of OpdB against unblocked peptides or peptides N-terminally blocked with a 3-(2-furyl)acryloyl moiety, reactions consisted of OpdB (18–50 fmol of active enzyme) in 50 mM Tris-Cl, 5 mM dithiothreitol, pH 8 (50 μl), prewarmed to 37 °C. Prewarmed substrate solution (50 μl) was added, and at timed intervals reactions were stopped and resolved by HPLC as described previously (10). The effect of pH on OpdB activity, the *K<sub>i</sub>* for non-tight binding reversible competitive inhibitors, and the *k<sub>a</sub>* for irreversible inhibitors were investigated as described previously (12). Degradation of atrial natriuretic factor (ANF) was studied by incubating rat ANF-(1–28) (Bachem), the predominant circulating form of ANF (31), at a 1:100 (mol:mol) OpdB:ANF ratio in 50 mM Tris-Cl, pH 8. At timed intervals, reaction products were resolved by reverse-phase high pressure liquid chromatography on a μBondpack C<sub>18</sub> column (Waters) eluted at a flow rate of 1 ml·min<sup>-1</sup> with a linear gradient of H<sub>2</sub>O:CH<sub>3</sub>CN:trifluoroacetic acid (95:5:0.1) increasing to H<sub>2</sub>O:CH<sub>3</sub>CN:trifluoroacetic acid (55:45:0.1) over 30 min, monitored at 214 nm. The ANF degradation products in HPLC fractions were identified by matrix-assisted laser desorption ionization time-of-flight (MALDI-TOF) as described previously (32).

**Detection of OpdB Activity in the Plasma of *T. evansi*-infected Rodents**—Adult male Sprague-Dawley rats (300 g; *n* = 4) were infected intraperitoneally with *T. evansi* IL3298 (1 × 10<sup>4</sup> trypanosomes/rat). At peak bloodstream parasitemia (≈ 5 × 10<sup>8</sup> trypanosomes·ml of plasma<sup>-1</sup>) blood was drawn from the tail vein (150 μl) into an equal volume of ice-cold 57 mM Na<sub>2</sub>HPO<sub>4</sub>, 3 mM NaH<sub>2</sub>PO<sub>4</sub>, 44 mM NaCl, 56 mM D(+)-glucose, 0.1 mM hypoxanthine, 2% (m/v) sodium citrate, pH 7.4, and centrifuged (1500 × *g*, 5 min, 4 °C). Supernatants were confirmed to be trypanosome-free by light microscopy. This procedure has previously been proven to yield parasite-free and cell-free plasma without destruction of live parasites in the plasma. Therefore, there is no artifactual extracellular release of intracellular trypanosome proteins (7). Plasma, similarly prepared from rats that had been "mock-infected" with 1 × 10<sup>4</sup> heat-killed trypanosomes/rat, was used as a control. The inhibitors 3,4-dichloroisocoumarin (DCI) and soybean trypsin inhibitor (SBTI) were used to discriminate serine oligopeptidase from trypsin-like serine protease activity, while activity-neutralizing anti-OpdB antibodies (7) were used to specifically detect OpdB activity. This combination of inhibitors is diagnostic for OpdB activity in complex biological fluids (7). For detection of immunoreactive OpdB in infected rat plasma, rats were euthanized at peak parasitemia, and blood was harvested by cardiac puncture and processed as described above. Whole plasma yielded poorly resolved bands on a Western blot; therefore, cell-free plasma was partially fractionated by precipitation and chromatography on Q-Sepharose and agmatine-Sepharose as described for purification of OpdB from *T. evansi* lysates. Fractionated plasma was resolved by SDS-PAGE and blotted for OpdB.

**Subcellular Fractionation of *T. evansi***—Subcellular fractionation was undertaken exactly as described previously (33). Briefly bloodstream-derived *T. evansi* trypomastigotes (10<sup>10</sup> cells) were washed in 0.25 M sucrose, 50 mM Hepes, 25 mM KCl, pH 7.4 at 4 °C and disrupted in a French pressure cell. Cell fractions (designated as "nuclear," "large granule," "small granule," "crude microsomal," and "soluble superna-

tant<sup>7</sup> fractions) were prepared by centrifugation as described previously (33). These fractions were screened for enrichment of fraction markers: hexokinase (a glycosome marker) (34),  $\alpha$ -mannosidase (a dense granule marker) (35), and alanine aminotransferase (a cytosol marker) (35) to evaluate the fractionation. Fractions were also screened for OpdB activity (measured as Cbz-Arg-Arg-AMC-hydrolyzing activity sensitive to inhibition by anti-OpdB IgY at 75  $\mu\text{g}\cdot\text{ml}^{-1}$ ).

**In Vitro Release of OpdB by *T. evansi***—Secretion of OpdB by *T. evansi* IL3298 *in vitro* was studied as described previously (6, 7). Bloodstream-derived *T. evansi* were resuspended ( $1 \times 10^8$  cells $\cdot\text{ml}^{-1}$ ) in minimal essential medium supplemented with 0.3 g $\cdot\text{liter}^{-1}$  L-glutamine, 0.25 mM L-cysteine, 0.01 mM bathocuproinedisulfonic acid, 15% (v/v) fetal bovine serum at 37 °C. Aliquots (100  $\mu\text{l}$ ) were removed at 0, 10, 30, and 60 min and centrifuged (1500  $\times g$  for 2 min at 4 °C). Trypanosome-free supernatants were assayed for activity against Cbz-Arg-Arg-AMC (5  $\mu\text{M}$ ) and N-succinyl-Gly-Pro-Leu-Gly-Pro-AMC (5  $\mu\text{M}$ ) as described above.

**A Rat Model of Lethal Endotoxic Shock**—Lethal endotoxic shock was induced in rats by slow (10-min) intravenous administration of 20 mg $\cdot\text{kg}^{-1}$  *E. coli* O127:B8 lipopolysaccharide (LPS; Sigma) via the tail vein (36). Rats generally expired between 9 and 16 h; therefore, plasma was harvested by cardiac puncture at 4 and 8 h post-LPS administration after which rats were sacrificed.

**Determination of Plasma ANF Levels**—Blood samples (0.5 ml) were extracted from the tail vein of rats 2 and 4 days preinfection, on the day of infection, and at 2-day intervals postinfection. Blood was extracted into an equal volume of ice-cold 57 mM  $\text{Na}_2\text{HPO}_4$ , 3 mM  $\text{NaH}_2\text{PO}_4$ , 44 mM NaCl, 56 mM D(+)-glucose, 0.1 mM hypoxanthine, 2% (m/v) sodium citrate, pH 7.4, supplemented with 2 mM DCI and centrifuged (1500  $\times g$  for 5 min at 4 °C). Plasma was first clarified on a  $\text{C}_{18}$  Sep-column (Bachem) after which plasma ANF levels were quantified with a rat ANF radioimmunoassay (Bachem) according to the manufacturer's instructions. Where necessary, larger quantities of blood were extracted from rats to bring the ANF levels within the detection limit of the assay (0.1–64 pg/tube).

**Half-life Determination for  $^{125}\text{I}$ -ANF**— $^{125}\text{I}$ -Tyr<sup>28</sup>ANF-(1–28) (Bachem; 2000 Ci $\cdot\text{mmol}^{-1}$ ) was incubated in trypanosome- and cell-free plasma from trypanosome-infected and healthy rats for 5 min. At 30-s intervals, aliquots were resolved by HPLC as described above. Radioactivity associated with the intact ANF peak was quantified in a  $\gamma$ -counter. A ratio was determined for the fraction of radiation recovered at time  $t$  ( $C_t$ ) representing intact ANF-(1–28) versus that initially applied ( $C_{\text{tot}}$ ). Linear regression of a semilog plot of  $\ln(C_t/C_{\text{tot}})$  versus time yielded a graph with a slope =  $k$  where  $k$  is the rate of disappearance of intact ANF. The half-life,  $t_{1/2}$ , is given by  $t_{1/2} = 0.693/k$ . For the estimation of ANF half-life in *T. evansi*-infected hosts, rats ( $\approx 300$  g) were selected at midlevel parasitemia (between days 6 and 8, postinfection; blood parasitemia  $\approx 10^7\cdot\text{ml}^{-1}$ ). Rats with higher parasitemia did not tolerate surgery and catheter placement. Rats were anesthetized with sodium pentobarbital (50 mg $\cdot\text{kg}^{-1}$ , intraperitoneal), and the left carotid artery and the right jugular vein were catheterized with PE-50 tubing. A bolus dose of  $^{125}\text{I}$ -Tyr<sup>28</sup>ANF-(1–28) (1  $\mu\text{Ci}$ ) was administered via the jugular catheter through which continuous infusion of Ringer's solution (50  $\mu\text{l}\cdot\text{min}^{-1}$ ) was maintained. At timed intervals (every 30 s for 5 min), arterial blood samples (0.5 ml) were extracted and processed for HPLC and  $\gamma$ -counting as described above. In some cases, either preimmune IgY or anti-OpdB IgY was infused via the jugular catheter at a rate of 17.5  $\mu\text{g}\cdot\text{min}^{-1}$  for 2 h prior to application of the  $^{125}\text{I}$ -Tyr<sup>28</sup>ANF-(1–28) bolus.

**Smooth Muscle Contraction Assay for ANF**—Adult male Sprague-Dawley rats ( $\approx 300$  g) were sacrificed by decapitation, and the aortas were extracted and placed in ice-cold Krebs-Henseleit solution (119.1 mM NaCl, 4.7 mM KCl, 1.2 mM  $\text{MgSO}_4$ , 1.2 mM  $\text{KH}_2\text{PO}_4$ , 25.0 mM  $\text{NaHCO}_3$ , 2.5 mM  $\text{CaCl}_2$ , and 5.5 mM D(+)-glucose) continuously gassed with 95% (v/v)  $\text{O}_2$ , 5% (v/v)  $\text{CO}_2$ . Adipose and connective tissue was gently removed, and the midthoracic region was cut into 2-mm sections. Aortic rings were mounted in a Mulvany myograph (J. P. Trading) in an organ bath for recording of isometric tension. Aortic rings were mounted on two 40- $\mu\text{m}$  stainless steel wires exactly as described previously (37) except that rings were precontracted with 10  $\mu\text{M}$  phenylephrine to estimate maximal force. Intact ANF-(1–28) was incubated with catalytically active or inactive OpdB at a 1:100 (mol:mol) OpdB:ANF ratio for 30 min. The reaction mixtures, containing 10  $\mu\text{M}$  to 10 pM ANF-(1–28) (either intact or fragmented by OpdB), OpdB alone (0.1  $\mu\text{M}$  to 0.1 pM, active concentration), or its catalytically inactive S563A variant (0.1  $\mu\text{M}$  to 0.1 pM by mass) were applied to the aortic rings. Ring contraction and relaxation were monitored continuously by a force displacement transducer coupled to a polygraph.

**Bioassay for ANF Prohypotensive Activity**—New Zealand White rabbits ( $\approx 3$  kg) were maintained under anesthesia by perfusion of 25

TABLE I  
Purification of OpdB from *T. evansi* TEVA1 lysates

Fraction	Activity	Specific activity	Purification	Yield
	$\text{pmol}\cdot\text{s}^{-1}$	$\text{pmol}\cdot\text{s}^{-1}\cdot\text{mg}^{-1}$	-fold	%
Lysate	2,008	24	1	100
TPP <sup>a</sup>	1,808	96	4	90
Q-Sepharose	1,668	181	8	83
Agmatine-Sepharose	1,302	692	29	65
Immunoaffinity	754	17,000	714	38

<sup>a</sup> TPP, three-phase partitioning.

mg $\cdot\text{ml}^{-1}$  ketamine, 1% (v/v) xylazine in 0.9% (m/v) NaCl infused at a rate of 8 ml $\cdot\text{h}^{-1}$  via a catheter in the left ear vein. Fluid replacement was undertaken with 0.9% (m/v) NaCl simultaneously infused at 20 ml $\cdot\text{h}^{-1}$  via the same catheter. The left carotid artery and right ear vein were catheterized and connected to pressure transducers for on-line monitoring of arterial and venous pressure. After 20–30 min of equilibration, a catalytically inactive OpdB(S563A) variant (10  $\mu\text{g}$ ) was applied as a bolus via a three-way stop-cock in the right ear vein catheter. Twenty minutes later wild-type OpdB (10  $\mu\text{g}$ ) was administered. In a different group of rabbits, rat ANF-(1–28) (8  $\mu\text{g}\cdot\text{kg}^{-1}$ ) was applied as a bolus via the right ear vein catheter after preincubation of ANF at a 1:100 (mol:mol) OpdB:ANF ratio with catalytically active or inactive OpdB variants for 30 min at 37 °C in 50 mM Tris-Cl, pH 8. Blood pressure was monitored continuously over the course of the experiment. Data presented are for a single rabbit but are representative of data from two other rabbits.

## RESULTS AND DISCUSSION

**Purification of OpdB**—Oligopeptidase B was purified from *T. evansi* lysates 714-fold in a four-step procedure with a 38% yield (Table I). The purified enzyme was 66% active as judged by active site titration. This is the first protease ever purified from *T. evansi*. Purified *T. evansi* OpdB was homogenous by reducing SDS-PAGE, yielding a single band at  $\sim 80$  kDa (Fig. 1). A band of comparable size was observed in Western blots of *T. evansi*, *T. brucei*, and *T. cruzi* lysates probed with anti-*T. brucei* OpdB antibodies (Fig. 1).

**Cloning and Sequencing of the *opdB* Gene**—The *opdB* gene isolated from *T. evansi* contained an open reading frame of 2148 bp encoding a polypeptide of 715 amino acids with a predicted molecular mass of 80.664 kDa. This is the first protease-encoding gene cloned and sequenced from *T. evansi*. The predicted molecular mass compares well with the size of the native enzyme purified from *T. evansi* lysates (Fig. 1). The *T. evansi opdB* gene exhibited a 99.4% identity with its *T. brucei* homologue, and their encoded proteins share 99.6% identity. The *T. evansi opdB* gene was present as a single copy per haploid genome as judged by Southern blot of endonuclease-restricted *T. evansi* genomic DNA probed with the full-length *opdB* coding sequence (Fig. 1). The *opdB* gene was expressed in *E. coli* as a soluble, catalytically active polyhistidine affinity-tagged enzyme with a protein yield of between 30 and 40 mg/liter of bacterial culture. The hyperexpressed protein yielded a single band on an SDS-polyacrylamide gel that migrated at a molecular mass corresponding to  $\sim 80$  kDa (Fig. 1).

**Kinetic Analysis of *T. evansi* OpdB**—There was little difference between the amidolytic activity of native, purified OpdB and His<sub>6</sub>-tagged recombinant OpdB against AMC peptide substrates, indicating that the affinity tag did not appreciably alter OpdB activity. The best substrate was Cbz-Arg-Arg-AMC ( $k_{\text{cat}}/K_m$  of 337  $\mu\text{M}^{-1}\cdot\text{s}^{-1}$ , comparing well with the 528  $\mu\text{M}^{-1}\cdot\text{s}^{-1}$  reported for OpdB from *T. brucei*) (12). This substrate also exhibited the lowest  $K_m$  (0.2  $\mu\text{M}$ ). No activity was observed against Cbz-Arg-Arg-AMC with the catalytically inactive OpdB variant in which the active site Ser<sup>563</sup> was converted to an Ala (see Fig. 1A). Basic residues were obligatory in P<sub>1</sub> and preferred (although not obligatory) in P<sub>2</sub> (nomenclature of Ref. 38) where hydrophobic residues as well as glycine and proline were

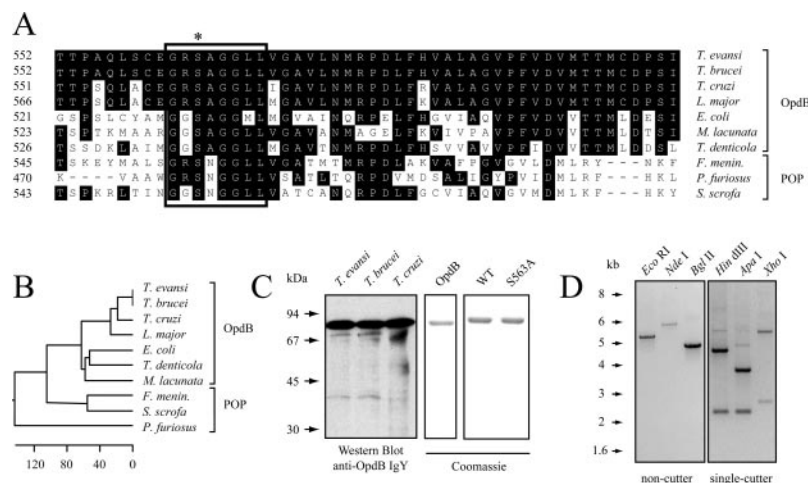


**FIG. 1. Oligopeptidase B from *T. evansi*.** *A*, multiple sequence alignment of the amino acid sequences surrounding the catalytic serine residue (\*) and the prolyl oligopeptidase family consensus sequence (boxed) for 10 members of the prolyl oligopeptidase family. Sequences were obtained from the GenBank<sup>TM</sup>/EBI data base under the following accession numbers: AF078916 (*T. brucei* OpdB), U69897 (*T. cruzi* OpdB), AF109875 (*Leishmania major* OpdB), D10976 (*E. coli* OpdB), D38405 (*Moraxella lacunata* OpdB), AAK39550 (*Treponema denticola* OpdB), D10980 (*Flavobacterium meningosepticum* (*F. menin*) prolyl oligopeptidase (POP)), U08343 (*Pyrococcus furiosus* prolyl oligopeptidase), and M64227 (*Sus scrofa* prolyl oligopeptidase). *B*, an unrooted dendrogram was prepared by comparing the full-length amino acid sequences using the ClustalW alignment software of the MEGALIGN program (DNASTAR). The scale at the bottom measures the distance between sequences. The units indicate the number of substitution events. *C*, lysates prepared from *T. evansi*, *T. brucei*, and *T. cruzi* (15  $\mu$ g) were resolved by reducing SDS-PAGE and probed with anti-*T. brucei* OpdB IgY (left panel). Oligopeptidase B purified from *T. evansi* extracts (2  $\mu$ g) (middle panel) and recombinant wild type (WT) and a catalytically dead variant (S563A) of *T. evansi* OpdB hyperexpressed in *E. coli* and affinity-purified on Ni<sup>2+</sup>-agarose (2  $\mu$ g) were resolved by reducing SDS-PAGE and visualized by Coomassie Blue staining (right panel). *D*, genomic DNA from *T. evansi* was digested with EcoRI, NdeI, and BglII (which do not cut within the *opdB* open reading frame) and HindIII, ApaI, and XhoI (which cut once within the *opdB* open reading frame). Digestions were resolved on a 0.8% agarose gel and transferred to a nylon membrane, and the *opdB* gene was detected with a <sup>32</sup>P-labeled DNA *opdB* probe.

**TABLE II**  
Amidolytic activity of OpdB from *T. evansi*

Substrate <sup>a</sup>	Native OpdB			Recombinant OpdB <sup>b</sup>		
	$K_m$	$k_{cat}$	$k_{cat}/K_m$	$K_m$	$k_{cat}$	$k_{cat}/K_m$
	$\mu$ M	$s^{-1}$	$s^{-1}\cdot\mu M^{-1}$	$\mu$ M	$s^{-1}$	$s^{-1}\cdot\mu M^{-1}$
Cbz-Arg-Arg-AMC	0.2	64	336.8	0.2	59	268.2
Boc-Leu-Arg-Arg-AMC	0.8	108	140.3	1.0	154	157.1
Boc-Leu-Lys-Arg-AMC	1.0	94	95.0	1.1	132	117.9
Boc-Gly-Arg-Arg-AMC	1.3	81	61.0	2.1	101	48.4
Boc-Ala-Arg-Arg-AMC	1.7	102	59.3	2.1	122	57.8
Boc-Leu-Gly-Arg-AMC	1.3	57	44.2	1.2	74	61.7
Boc-Gly-Lys-Arg-AMC	1.9	76	39.6	1.2	55	43.0
Cbz-Phe-Arg-AMC	2.3	59	26.5	3.0	77	23.5
Boc-Val-Gly-Arg-AMC	3.0	64	21.1	2.1	58	27.2
Boc-Val-Leu-Lys-AMC	3.0	18	5.9	4.4	22	5.0
H-Ala-Phe-Lys-AMC	4.4	23	5.2	5.0	34	6.8
Cbz-Arg-AMC	4.0	17	4.3	3.0	26	8.6
Boc-Ala-Gly-Pro-Arg-AMC	13.5	12	0.9	10.2	9	0.8
Boc-Val-Pro-Arg-AMC	12.2	8	0.7	14.3	12	0.8
H-Arg-AMC	40.0	1	0.03	48.0	2	0.05
Cbz-Gly-Gly-Arg- $\beta$ NA	2.9	48	16.6	3.3	33	10.0
H-Arg-Arg- $\beta$ NA	2.4	30	12.5	2.0	21	10.5
H-Phe-Arg- $\beta$ NA	3.8	18	4.7	4.9	17	3.5
H-Gly-Arg- $\beta$ NA	4.8	12	2.5	4.7	11	1.9

<sup>a</sup> No degradation of *N*-succinyl-Gly-Pro-Leu-Gly-Pro-AMC, glutaryl-Gly-Phe-AMC, H-Gly-Pro-AMC, or H-Asp-Arg- $\beta$ NA was observed. The S.E. of the  $K_m$  was within 5% ( $n = 3$ ). Boc, *t*-butoxycarbonyl.

<sup>b</sup> The active site-mutated recombinant OpdB(S563A) exhibited no activity against Cbz-Arg-Arg-AMC (5  $\mu$ M) or *t*-butoxycarbonyl-Leu-leu-Arg-AMC (5  $\mu$ M) under the same conditions.

also accepted (Table II). A range of residues was also accepted in  $P_3$  (hydrophobic > small, uncharged; Table II). Thus, the *T. evansi* OpdB substrate specificity parallels that of *T. brucei* OpdB (12). While displaying poor arginyl aminopeptidase activity, OpdB displayed a strong arginyl carboxypeptidase activity (Table III), which has previously been identified by Hemerly *et al.* (32) but which has not been characterized for any OpdB to date. Oligopeptidase B liberated Arg<sup>4</sup> from H-Val<sup>1</sup>-Lys<sup>2</sup>-Arg<sup>3</sup>-Arg<sup>4</sup>-OH with a  $k_{cat}/K_m$  of 231.6  $s^{-1}\cdot mM^{-1}$  and a  $K_m$

**TABLE III**  
Carboxypeptidase activity of OpdB from *T. evansi*

Substrate <sup>a</sup>	Native OpdB			Recombinant OpdB		
	$K_m$	$k_{cat}$	$k_{cat}/K_m$	$K_m$	$k_{cat}$	$k_{cat}/K_m$
	mM	$s^{-1}$	$s^{-1}\cdot mM^{-1}$	mM	$s^{-1}$	$s^{-1}\cdot mM^{-1}$
H-Val-Lys-Arg $\downarrow$ Arg-OH <sup>b</sup>	0.2	44	232	0.3	38	127
H-Arg-Arg $\downarrow$ Arg-OH	0.6	38	60	1.1	29	27
H-Gly-Gly-Lys $\downarrow$ Arg-OH	1.6	54	33	2.2	40	18
FA-Tyr-Lys $\downarrow$ Arg-OH	1.1	18	15	1.9	12	6
H-Phe-Arg $\downarrow$ Arg-OH	2.7	21	8	3.0	16	5

<sup>a</sup> No degradation of the following substrates (20 mM) was observed over a 30-min time course: H-Arg-Arg-OH and H-Lys-Arg-OH. The scissile bond is indicated with  $\downarrow$ . The S.E. of the  $K_m$  was within 7% of the mean of three independent determinations. FA, 3-(2-furyl)acryloyl.

<sup>b</sup> Prolonged incubation of this substrate (>15 min) yielded a secondary cleavage at Lys  $\downarrow$  Arg.

of 0.19 mM with liberation of Arg<sup>3</sup> upon prolonged incubation (>15 min; not shown). Shortening the peptide to H-Arg<sup>1</sup>-Arg<sup>2</sup>-Arg<sup>3</sup>-OH, OpdB liberated Arg<sup>3</sup> generating H-Arg-Arg-OH and H-Arg-OH with a  $k_{cat}/K_m$  of 60  $s^{-1}\cdot mM^{-1}$  and a  $K_m$  of 0.63 mM. No further degradation of H-Arg-Arg-OH to two H-Arg-OH molecules occurred, and when H-Arg-Arg-OH was supplied as the sole substrate, no hydrolysis of the Arg-Arg bond was observed, perhaps indicating that at least both  $P_1$  and  $P_2$  must be occupied in addition to  $P_1$ , for carboxypeptidase activity to proceed (*i.e.* the Arg-Arg dipeptide was too short). Both Arg and Lys were acceptable in  $P_1$  for carboxypeptidase activity, and both Phe and Tyr were acceptable in  $P_2$ . Thus, the same  $P_1$  and  $P_2$  preferences were exhibited for arginyl carboxypeptidase activity as were apparent for amidolytic (endopeptidase) activity (Table II).

Oligopeptidase B was rapidly inactivated by DCI ( $k_a = 224 \pm 28 M^{-1}\cdot s^{-1}$ ); therefore we used this inhibitor in our physiological experiments. The monobasic inhibitors benzamidine and agmatine were poor OpdB inhibitors ( $K_i \approx 200 \mu$ M), explaining why agmatine is a poor affinity ligand in our purification protocol (Table I) since OpdB eluted from agmatine-Sepharose at low (150 mM) salt concentrations. High molecular mass inhib-

TABLE IV  
Inhibitor profile of OpdB from *T. evansi*

Inhibitor <sup>a</sup>	Native OpdB	Recombinant OpdB
Irreversible inhibitors ( $k_a$ ( $M^{-1}s^{-1}$ ) $\pm$ S.D.)		
3,4-Dichloroisocoumarin	224 $\pm$ 28	273 $\pm$ 41
4-(2-Aminoethyl)benzenesulfonyl fluoride	60 $\pm$ 6	72 $\pm$ 9
Phenylmethanesulfonyl fluoride	0.04 $\pm$ 0.01	0.17 $\pm$ 0.03
Reversible inhibitors ( $K_i$ ( $\mu M$ ) $\pm$ S.D.)		
Antipain	2 $\pm$ 0.2 $\times 10^{-3}$	1 $\pm$ 0.1 $\times 10^{-3}$
Leupeptin	21 $\pm$ 4 $\times 10^{-3}$	29 $\pm$ 7 $\times 10^{-3}$
Benzamidine	218 $\pm$ 36	254 $\pm$ 45
Agmatine	188 $\pm$ 13	207 $\pm$ 30

<sup>a</sup> No inhibitory activity was observed for soybean trypsin inhibitor (100  $\mu g \cdot ml^{-1}$ ), turkey ovomucoid (100  $\mu g \cdot ml^{-1}$ ),  $\alpha_1$ -proteinase inhibitor (50  $\mu g \cdot ml^{-1}$ ),  $\alpha_2$ -antiplasmin (50  $\mu g \cdot ml^{-1}$ ), or antithrombin III (25  $\mu g \cdot ml^{-1}$ ).

itors of serine peptidases (serpins), including SBTI, ovomucoid,  $\alpha_1$ -proteinase inhibitor,  $\alpha_2$ -antiplasmin, and antithrombin III, did not inhibit OpdB (Table IV). The lack of effect of these serpins is attributable to the presence of a  $\beta$ -propeller domain at the N terminus of these oligopeptidases (39) that acts as a steric gate that restricts access to the OpdB active site, allowing only oligopeptides to reach the substrate binding and catalytic machinery. This steric gate also prevents these high molecular mass serpins from forming inhibitory complexes with OpdB (40). This inability of mammalian plasma peptidase inhibitors to inhibit OpdB activity is important since, upon release by parasites into the host circulation, OpdB would retain catalytic activity. Along these lines, OpdB is not only active but is also maximally stable at the pH of the host plasma (Fig. 2A). These data are consistent with an enzyme located in the trypanosome cytoplasm. Indeed OpdB of *T. cruzi* has been localized to the parasite cytosol (14).

**Extracellular Release of OpdB**—Upon *in vitro* incubation of *T. evansi*, no release of Cbz-Arg-Arg-AMC-hydrolyzing activity into the medium was observed, although secretion of a N-succinyl-Gly-Pro-Leu-Gly-Pro-AMC-hydrolyzing activity (marker for a secreted trypanosome prolyl oligopeptidase (6)) was evident (Fig. 2B). Our subcellular fractionation studies further indicated that OpdB was located in the trypanosome cytosol since OpdB activity was enriched only in the high speed soluble supernatant that contains the cytosolic fraction as evident from the enrichment in alanyl aminopeptidase activity, a cytosolic marker (35) (Fig. 2E). No enrichment of OpdB activity was observed in granule or in nuclear/debris fractions (Fig. 2E). These observations are consistent with the lack of a secretion signal in the OpdB sequence and the cytosolic localization of the *T. cruzi* OpdB homologue (14). In contrast, cell-free plasma of infected rodents displayed a potent Cbz-Arg-Arg-AMC-hydrolyzing activity that was absent in mock-infected rodents (Fig. 2C). This activity was inhibited by DCI (which inhibits both serine proteases and serine oligopeptidases) but was insensitive to SBTI (which only inhibits serine proteases but not serine oligopeptidases), thus implicating a serine oligopeptidase. This combination of substrate and inhibitors is diagnostic for OpdB (7). Activity-neutralizing anti-OpdB antibodies abrogated this activity, while preimmune antibodies at the same concentration did not, suggesting that OpdB was released by parasites into the host bloodstream (Fig. 2C). In support of this, bloodstream parasitemia correlated well ( $r^2 = 0.87$ ) with OpdB activity in the plasma of *T. evansi*-infected rats (Fig. 2D). Using the same combination of inhibitors in rats treated with a lethal dose of LPS, no OpdB-like activity was observed in the acute phase plasma of rats in endotoxic shock. Indeed a small (2–3-fold) increase in Cbz-Arg-Arg-AMC-hydrolyzing activity was observed in LPS-treated rats 8 h post-LPS administration (Fig. 2C); however, this activity was inhibited by SBTI and was not inhibited by anti-OpdB IgY. Taken together, these data indicate that the Cbz-Arg-Arg-AMC-hydrolyzing activity that is

increased in the plasma of LPS-treated rats was not an OpdB-like activity, although it can also be attributed to a trypsin-like serine peptidase. Peptidases of the extrinsic coagulation pathway are activated in animal models of LPS-induced endotoxic shock (41), and it is likely that one of these peptidases is responsible for this activity. Immunoreactive OpdB was evident in cell-free plasma of *T. evansi*-infected rodents but was absent in mock-infected rodents (Fig. 3). No OpdB immunoreactivity was observed in plasma from rats treated with a lethal dose of LPS at 4 and 8 h post-LPS administration (results not shown). Together these data suggest that the OpdB present in the plasma of infected hosts is released *in vivo* by dead or dying trypanosomes that are lysed in the host circulation by the various antimicrobial host defense mechanisms.

**Cleavage of ANF by OpdB *In Vitro***—Given the high  $k_{cat}$  for the amidolytic (up to 108  $s^{-1}$ ) and carboxypeptidase (up to 54  $s^{-1}$ ) activity of OpdB, its presence in the host plasma has serious implications for the pathogenesis of surra particularly since this enzyme is active and optimally stable at the pH of the blood (Fig. 2A) and is not regulated by endogenous plasma peptidase inhibitors (Table IV). Unregulated OpdB activity in the bloodstream could influence peptide hormone homeostasis in the host, an idea supported by the observed reductions in circulating levels of peptide hormones, such as ANF, in the plasma of dogs infected with African trypanosomes (17). It seemed possible that OpdB could be responsible for these reduced ANF levels since the ANF primary sequence contains five putative OpdB cleavage sites (Table V). Co-incubation of OpdB and ANF-(1–28), the major circulating form of ANF in the rat (31), generated four cleavage products that were separated by reverse-phase HPLC (Table V). No cleavage occurred at the Arg-Ile bond in Asp<sup>13</sup>Arg<sup>14</sup>Ile<sup>15</sup>, probably due to the acidic Asp<sup>13</sup> residue in P<sub>2</sub>, since H-Asp-Arg- $\beta$ NA was not cleaved by OpdB either (Table II). However, MALDI-TOF analysis of the reduced HPLC-purified fragments indicated cleavage at Leu<sup>2</sup>Arg<sup>3</sup>↓Arg<sup>4</sup>, Arg<sup>3</sup>Arg<sup>4</sup>↓Ser<sup>5</sup>, Gly<sup>10</sup>Arg<sup>11</sup>↓Ile<sup>12</sup>, and Phe<sup>26</sup>Arg<sup>27</sup>↓Tyr<sup>28</sup>.

Structure-activity relationships with ANF indicate that loss of Arg<sup>4</sup> generates a truncated ANF analogue with a 10-fold reduction in natriuretic activity (42) and a 7-fold reduction in vasorelaxant activity (43). Loss of Arg<sup>3</sup> has less effect, causing a 3-fold decrease in vasorelaxant properties (43). Thus, the Leu<sup>2</sup>Arg<sup>3</sup>↓Arg<sup>4</sup>↓Ser<sup>5</sup> cleavages by OpdB are likely to have physiological significance. In contrast, loss of Tyr<sup>28</sup> (which is also observed with OpdB; Table V) does not alter vasorelaxation properties of ANF (43), but removal of both Arg<sup>4</sup> and Tyr<sup>28</sup> together have additive deleterious effects (43). Therefore, processing of ANF by OpdB at all of these sites would be physiologically relevant. Preservation of the ANF ring structure is also critical for ANF bioactivity, and cleavage within the ring region at Asp<sup>13</sup> by a *Staphylococcus* protease abolishes ANF vasorelaxant activity (44). Indeed cleavage within the ANF ring at Cys<sup>7</sup>↓Phe<sup>8</sup>, which leaves the disulfide bridge

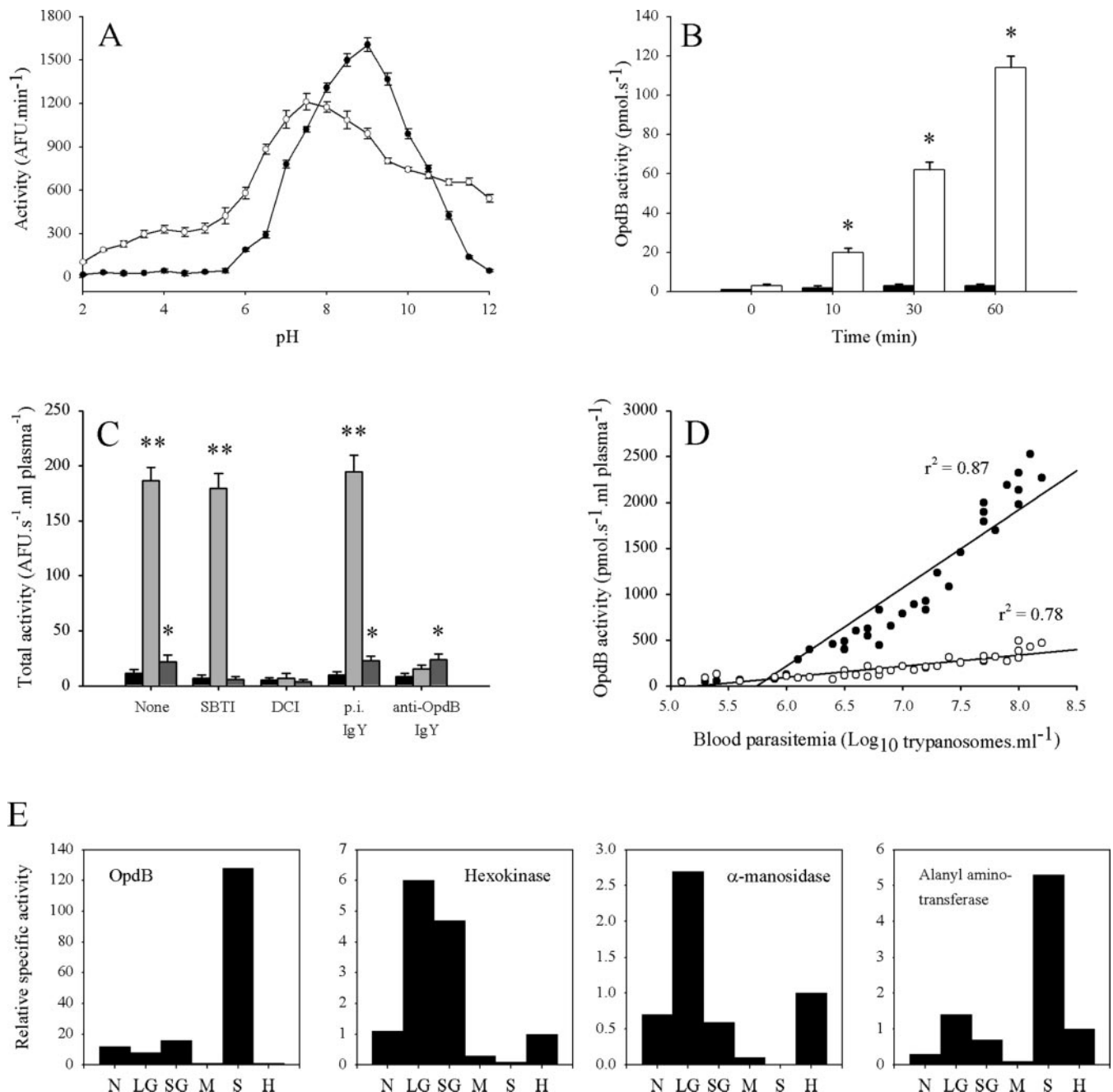


**FIG. 2. Oligopeptidase B is released by *T. evansi* into the host circulation.** A, effect of pH on the activity (■) and stability (□) of *T. evansi* OpdB evaluated against Cbz-Arg-Arg-AMC in constant ionic strength acetate-Mes-Tris buffers at 37 °C. B, *T. evansi* were resuspended ( $1 \times 10^8$  cells·ml<sup>-1</sup>) in defined medium as described under “Material and Methods” at 37 °C. Aliquots (100 μl) were removed at 0, 10, 30, and 60 min; centrifuged; and assayed for amidolytic activity against substrates for OpdB (Cbz-Arg-Arg-AMC; closed bars) and prolyl oligopeptidase (N-succinyl-Gly-Pro-Leu-Gly-Pro-AMC; open bars). Data reflect the mean activity (pmol·s<sup>-1</sup>) ± S.D. ( $n = 3$ ) of a 100-μl aliquot of trypanosome-free medium normalized for background (the same activity in a 100-μl aliquot of medium to which no trypanosomes had been added). \*,  $p < 0.001$  between the indicated data point and the corresponding value at the previous time point. C, plasma harvested from healthy (closed bars), *T. evansi*-infected rats at peak parasitemia ( $1 \times 10^8$  trypanosomes·ml<sup>-1</sup>; 10–12 days postinfection) (light gray bars), or LPS-treated rats 8 h post-LPS administration (dark gray bars) was assayed for activity against Cbz-Arg-Arg-AMC in the presence of SBTI (100 μg·ml<sup>-1</sup>), DCI (1 mM), or 250 μg·ml<sup>-1</sup> preimmune IgY or anti-OpdB IgY. \*,  $p < 0.05$ ; \*\*,  $p < 0.001$  compared with untreated plasma. D, plasma from *T. evansi*-infected rats was assayed over the course of an infection for amidolytic activity against Cbz-Arg-Arg-AMC in the presence of 250 μg·ml<sup>-1</sup> non-immune (●) or anti-OpdB (○) IgY. In B and D, “OpdB activity” reflects the activity observed in the presence of SBTI (100 μg·ml<sup>-1</sup>). E, subcellular fractionation of *T. evansi* cell bodies into crude nuclear (N), large granule (LG), small granule (SG), crude microsomal (M), and high speed soluble supernatant (S). The specific activities of marker enzymes and OpdB are described relative to the specific activity of the homogenate (H). AFU, arbitrary fluorescence units; p.i., pre-immune.

intact, is the primary ANF degradative cleavage occurring in the renal brush border (45). We illustrate in Table V that OpdB also cleaves ANF within the ring structure at Gly<sup>10</sup>Arg<sup>11</sup> ↓ Ile<sup>12</sup>. In summary, OpdB can cleave ANF at four distinct sites, all of which may render ANF either partly or completely biologically inactive. Therefore, two bioassays were used to evaluate the *in vitro* and *in vivo* effects of ANF cleavage by OpdB.

**Cleavage by OpdB Abrogates ANF Biological Activity—***In vitro* incubation of ANF with OpdB at 1:100 (mol:mol) OpdB:ANF ratios for 30 min abrogated the vasorelaxant capacity of ANF as evaluated by an aortic ring relaxation assay since no aortic ring relaxation was observed (Fig. 4). In contrast, ANF incubated at the same ratio with a catalytically inactive OpdB(S563A) variant retained full vasorelaxant properties, causing  $84 \pm 4\%$  relaxation



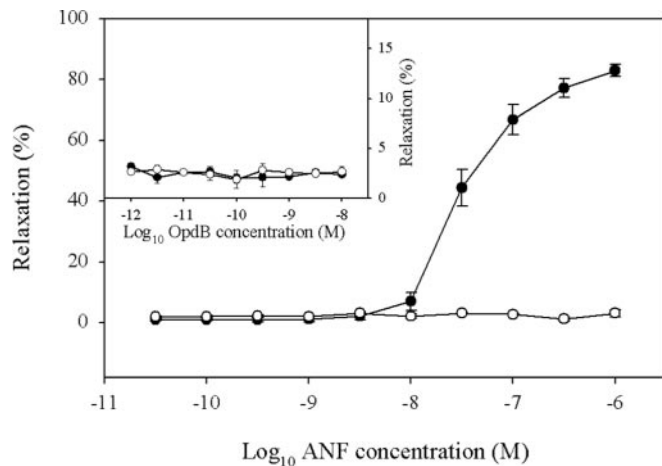


**FIG. 4. Oligopeptidase B abrogates the vasorelaxant properties of ANF.** Rat ANF-(1–28) preincubated with catalytically active OpdB (○) or a catalytically inactive OpdB(S563A) variant (●) was applied to aortic rings precontracted with 10  $\mu$ M phenylephrine. Data represent the percentage of relaxation relative to uncontracted rings and are indicated by the mean  $\pm$  S.E. ( $n = 3$ ). \*,  $p < 0.001$  between ● and ○ groups at the same ANF concentration. Both wild-type (○) and catalytically inactive OpdB (●) had no intrinsic vasorelaxant properties at the doses used in this study (inset).

In plasma from LPS-challenged rats, drawn at 4 and 8 h after LPS challenge, the ANF  $t_{1/2}$  was slightly elevated to  $\sim 90$  and 100 min, respectively (Fig. 7B and G). Thus, no ANF-hydrolyzing peptidases appeared to be induced in a rodent model of endotoxic shock. These data are consistent with our observations that ANF levels are not reduced after lethal LPS challenge (Fig. 6D). However, addition of the broad spectrum irreversible serine peptidase inhibitor DCI increased the ANF  $t_{1/2}$  in plasma from healthy rats a meager 1.5-fold to  $122 \pm 25$  min, indicating that host plasma serine peptidases were able to degrade ANF albeit very slowly. In plasma from *T. evansi*-infected rats, DCI increased the plasma ANF  $t_{1/2}$  a dramatic 250-fold from  $0.32 \pm 0.20$  to  $82 \pm 22$  min (Fig. 7, C and G). These data indicate that it was primarily a serine peptidase in the plasma from *T. evansi*-infected rats that was responsible for the rapid ANF turnover. However, in plasma from *T. evansi*-infected rats, DCI was not able to elevate the ANF  $t_{1/2}$  to that observed in DCI-treated plasma from healthy rats ( $122 \pm 25$  min). Thus, other DCI-insensitive peptidases (and thus, probably not serine peptidases) present in the plasma of *T. evansi*-infected rats were also able to hydrolyze ANF. Exogenous addition of recombinant OpdB to whole plasma from healthy rats (to an activity of  $2500 \text{ pmol}\cdot\text{s}^{-1}\cdot\text{ml of plasma}^{-1}$ , which approximates the activity observed in plasma from rats at high parasitemia) caused a dramatic decrease in the ANF  $t_{1/2}$  (down to 0.99 min) in comparison with that observed when a catalytically inactive OpdB(S563A) variant was added to the healthy plasma instead (ANF  $t_{1/2} = 85$  min; Fig. 7D). These data suggest that OpdB, in whole plasma, can indeed modulate the ANF  $t_{1/2}$  *in vitro*. In addition to the serine peptidase inhibitor DCI, we also used two potent inhibitors of trypanosome cysteine peptidases to investigate whether trypanosome cysteine peptidases that may be released by trypanosomes in the bloodstream can also modulate ANF levels in the plasma. Bloodstream-form African trypanosomes express both cathepsin L-like and cathepsin B-like cysteine peptidases with the latter being up-regulated in bloodstream-form parasites (52), and the Arg<sup>3</sup>Arg<sup>4</sup>Ser<sup>5</sup> region of ANF would be particularly susceptible to attack by cathepsin B-type enzymes. The broad spectrum cysteine peptidase inhibitor *L*-trans-epoxysuccinyl-L-leucyl-amido(4-guanidino)butane (E-64) was used at 10  $\mu$ M, which is

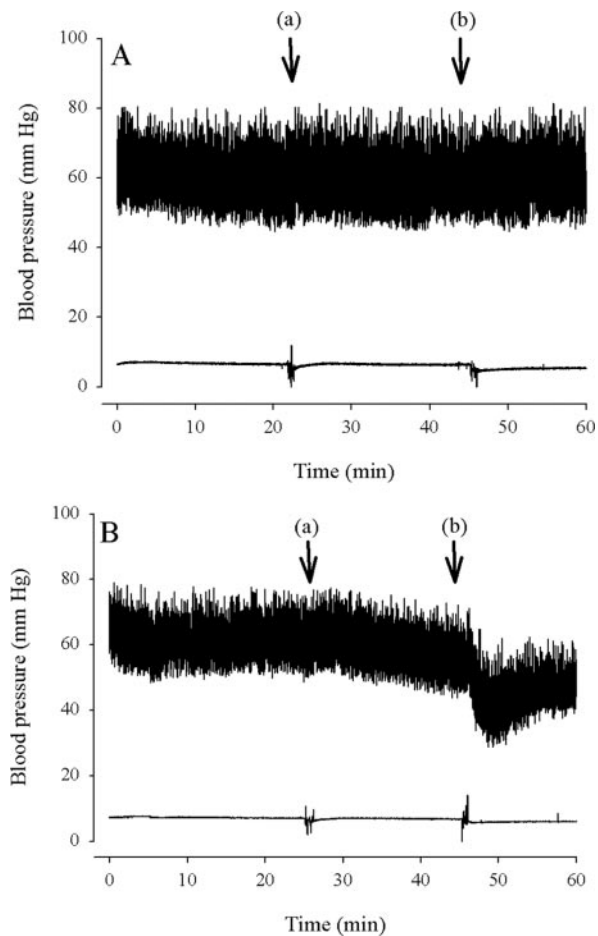


**FIG. 5. Oligopeptidase B abrogates the prohypotensive properties of ANF.** A, a catalytically inactive OpdB variant (a; 10- $\mu$ g bolus) followed by a wild-type, catalytically active (b; 10- $\mu$ g bolus) OpdB was applied directly to the rabbit circulation via the right ear vein as indicated, while arterial (upper trace in each panel) and venous (lower trace in each panel) blood pressure was monitored by catheters in the left carotid and right ear vein. B, similarly, rat ANF-(1–28) incubated with wild-type, catalytically active OpdB (a) and a catalytically inactive OpdB(S563A) variant (b) at 1:100 ratios (mol:mol) OpdB:ANF for 30 min was applied to the rabbit circulation via the right ear vein as indicated. The spikes on the venous pressure traces occur during the administration of the agents since they are administered via the pressure sensor catheter and thus do not indicate changes to venous pressure.

sufficient to completely inhibit cysteine peptidases from African trypanosomes (10); although it is without activity against OpdB, which, atypically for serine peptidases, is also inhibited by E-64 albeit at much higher concentrations ( $K_i$  for OpdB, 62  $\mu$ M (12)). In plasma from *T. evansi*-infected rats, the ANF  $t_{1/2}$  was unchanged ( $\sim 0.29$  min) in the presence or absence of E-64 (Fig. 7, A and E, compare closed boxes). Similarly in the presence of 100  $\mu$ M Cbz-Phe-Ala-diazomethyl ketone (CHN<sub>2</sub>), a potent ( $k_a = 6.5 \times 10^5 \text{ M}^{-1}\cdot\text{s}^{-1}$  (53)) inhibitor of trypanosome cysteine peptidases, there was no significant difference in the ANF  $t_{1/2}$ , which remained stable around 0.26 min in the plasma from *T. evansi*-infected rats (Fig. 7, compare A and F). Thus, we conclude from these data that cysteine peptidases from *T. evansi* do not alter ANF stability in the plasma.

Incubation of plasma from healthy rats with anti-OpdB antibodies did not appreciably alter the ANF  $t_{1/2}$  (Fig. 8, A and E) in comparison with control plasma to which no antibodies were added (Fig. 7, A and G). However, anti-OpdB antibodies increased the ANF  $t_{1/2}$  in plasma from *T. evansi*-infected rats 230-fold from  $0.32 \pm 0.20$  (Fig. 7, A and G) to  $73 \pm 18$  min (Fig. 8, A and E). Since these anti-OpdB antibodies potently and

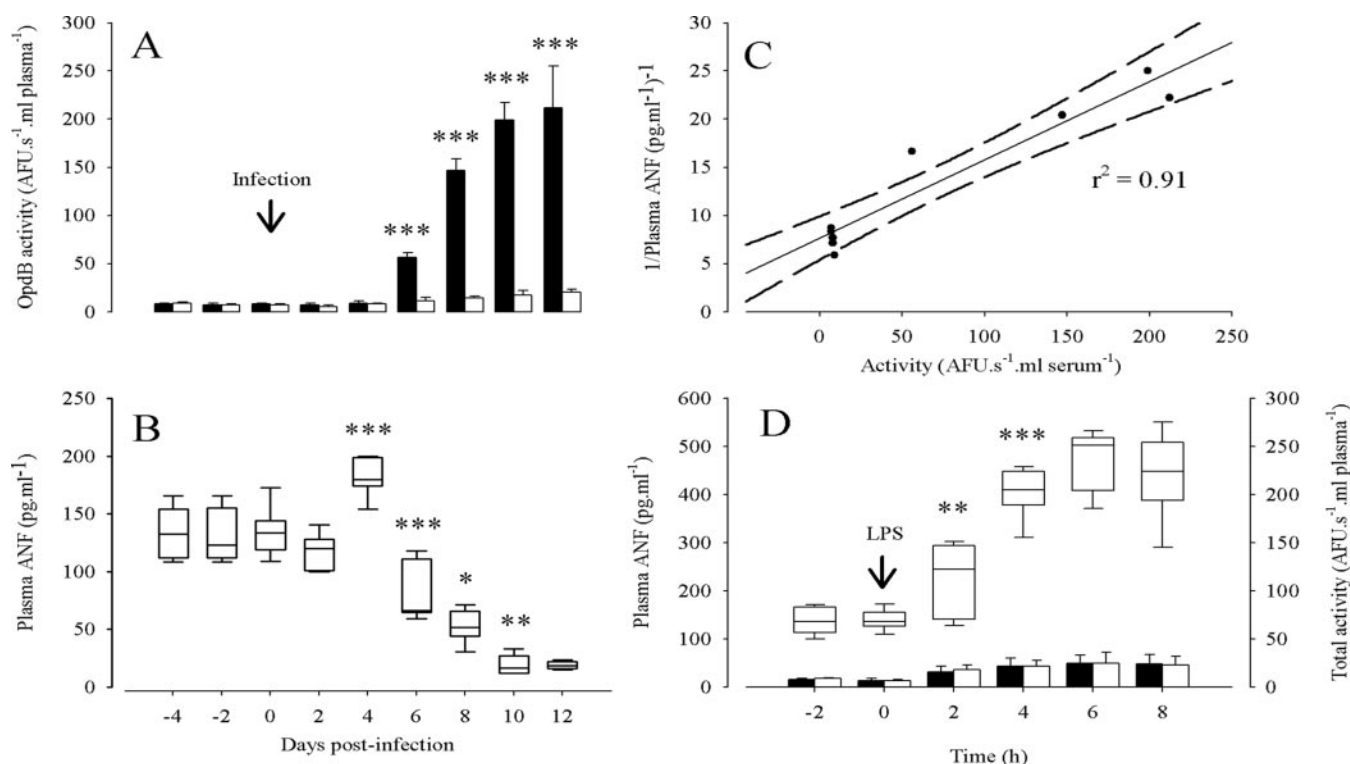


**FIG. 6. Plasma OpdB and plasma ANF levels are inversely correlated.** A, the OpdB activity was determined in the plasma of *T. evansi*-infected rats ( $n = 6$ ) in the presence of  $250 \mu\text{g}\cdot\text{ml}^{-1}$  preimmune (open bars) and anti-OpdB (closed bars) IgY as described under "Materials and Methods." \*\*\*,  $p < 0.001$  between open and closed bars on the same day postinfection. B, plasma ANF levels in rats infected with *T. evansi* were determined by radioimmunoassay from blood samples taken 2 and 4 days prior to intraperitoneal infection and at 2-day intervals postinfection. The bars represent the data range, while the boxes represent lower and upper quartiles. The line within the quartile box indicates the median ( $n = 6$ ). \*,  $p < 0.05$ ; \*\*,  $p < 0.005$ ; and \*\*\*,  $p < 0.001$ , comparing a data point to the previous data point (i.e. 2 days earlier). C, an inverse correlation exists between circulating plasma ANF levels and plasma OpdB activity. Dashed lines indicate the 95% confidence intervals. D, plasma ANF levels in rats challenged with a lethal dose of LPS to induce endotoxic shock were determined by radioimmunoassay from blood samples taken 2 h prior to intravenous application of LPS ( $20 \text{ mg}\cdot\text{kg}^{-1}$ ) and at 2-h intervals postinfection. The bars represent the data range, while the boxes represent lower and upper quartiles. The line within the quartile box indicates the median ( $n = 4$ ). \*\*,  $p < 0.005$ ; and \*\*\*,  $p < 0.001$ , comparing a data point to the previous data point (i.e. 2 h earlier). On the same axes, Cbz-Arg-Arg-AMC-hydrolyzing activity was determined in the plasma of LPS-challenged rats ( $n = 4$ ) in the presence of  $250 \mu\text{g}\cdot\text{ml}^{-1}$  preimmune (open bars) and anti-OpdB (closed bars) IgY as described under "Materials and Methods." Differences between open and closed bars on the same day postchallenge were not significant ( $p > 0.05$ ). AFU, arbitrary fluorescent units.

specifically inhibit OpdB activity without inhibiting the activity of plasma serine peptidases (7), OpdB appears to be primarily responsible for the dramatically decreased ANF  $t_{1/2}$  in plasma from *T. evansi*-infected rats. A parallel situation was observed when these antibodies were used after affinity purification on OpdB-Sepharose. The potency of the antibody preparation was considerably increased since at  $15 \mu\text{g}\cdot\text{ml}^{-1}$  the ANF  $t_{1/2}$  in plasma from *T. evansi*-infected rats was restored to that observed in plasma from uninfected rats (74 min; Fig. 8, B and E). Preimmune serum at the same concentration did not elevate ANF  $t_{1/2}$  in *T. evansi*-infected rat plasma, which remained at 0.34 min (Fig. 8, B and E). Since these anti-OpdB antibodies are monospecific for OpdB and do not neutralize the activity of other plasma serine peptidases including, *inter alia*, mast cell tryptase, kallikrein, plasmin, thrombin, and factor Xa (7), these data strongly suggest that OpdB in the plasma of *T. evansi*-infected rats is largely responsible for ANF degradation. In support of this idea, exogenous addition of catalytically active OpdB and activity-neutralizing anti-OpdB antibodies together to plasma from healthy rats yielded an ANF plasma half-life of  $70 \pm 12$  min, which is comparable to control values in healthy rat plasma. However, when the anti-OpdB antibodies were replaced with preimmune antibodies, the plasma ANF  $t_{1/2}$  was reduced 77-fold to  $0.9 \pm 0.30$  min (antibodies at  $250 \mu\text{g}\cdot\text{ml}^{-1}$ ; Fig. 8, C and E), approximating that obtained when catalytically active OpdB alone was added to healthy rat plasma (ANF  $t_{1/2}$  of  $0.99 \pm 0.29$  min; Fig. 7, D and G). To explore

whether host peptidases that may be induced during systemic inflammation could contribute to the ANF degradation that we observed, a rat model of LPS-induced lethal endotoxic shock was used. The ANF  $t_{1/2}$  was determined in the presence of preimmune or anti-OpdB IgY in plasma that was extracted from rats 8 h post-LPS challenge. Both in the presence of anti-OpdB IgY and in the presence of preimmune IgY at  $250 \mu\text{g}\cdot\text{ml}^{-1}$  (Fig. 8, D and E), the ANF  $t_{1/2}$  was unchanged when compared with the ANF  $t_{1/2}$  in plasma from healthy rats (Fig. 7, A and G). The same result was obtained using affinity-purified anti-OpdB IgY and preimmune IgY at  $15 \mu\text{g}\cdot\text{ml}^{-1}$  (results not shown). Taken together, these data confirm that trypanosome-derived OpdB in the plasma can modulate the ANF  $t_{1/2}$  *in vitro*.

To explore this idea *in vivo*, [ $^{125}\text{I}$ -Tyr $^{28}$ ]ANF-(1-28) was administered intrajugularly to healthy and to *T. evansi*-infected rats at midlevel parasitemia, and the intact [ $^{125}\text{I}$ -Tyr $^{28}$ ]ANF-(1-28) in arterial blood samples was determined at 30-s intervals postadministration. In healthy rats, the ANF  $t_{1/2}$  was  $1.1 \pm 0.26$  min (Fig. 7, F and H), which falls well within the range reported by other investigators using the same technique in healthy rats: 0.5 (54) to 2.1 min (55). However, in *T. evansi*-infected animals, the plasma ANF  $t_{1/2}$  was reduced 5-fold to  $0.24 \pm 0.15$  min (Fig. 9, A and C). Thus, intact live animals infected with *T. evansi* also display faster ANF turnover. The very low  $t_{1/2}$  observed in *T. evansi*-infected rats is probably attributable to the combined effects of plasma OpdB, membrane-bound neutral endopeptidase, and ANF clearance recep-

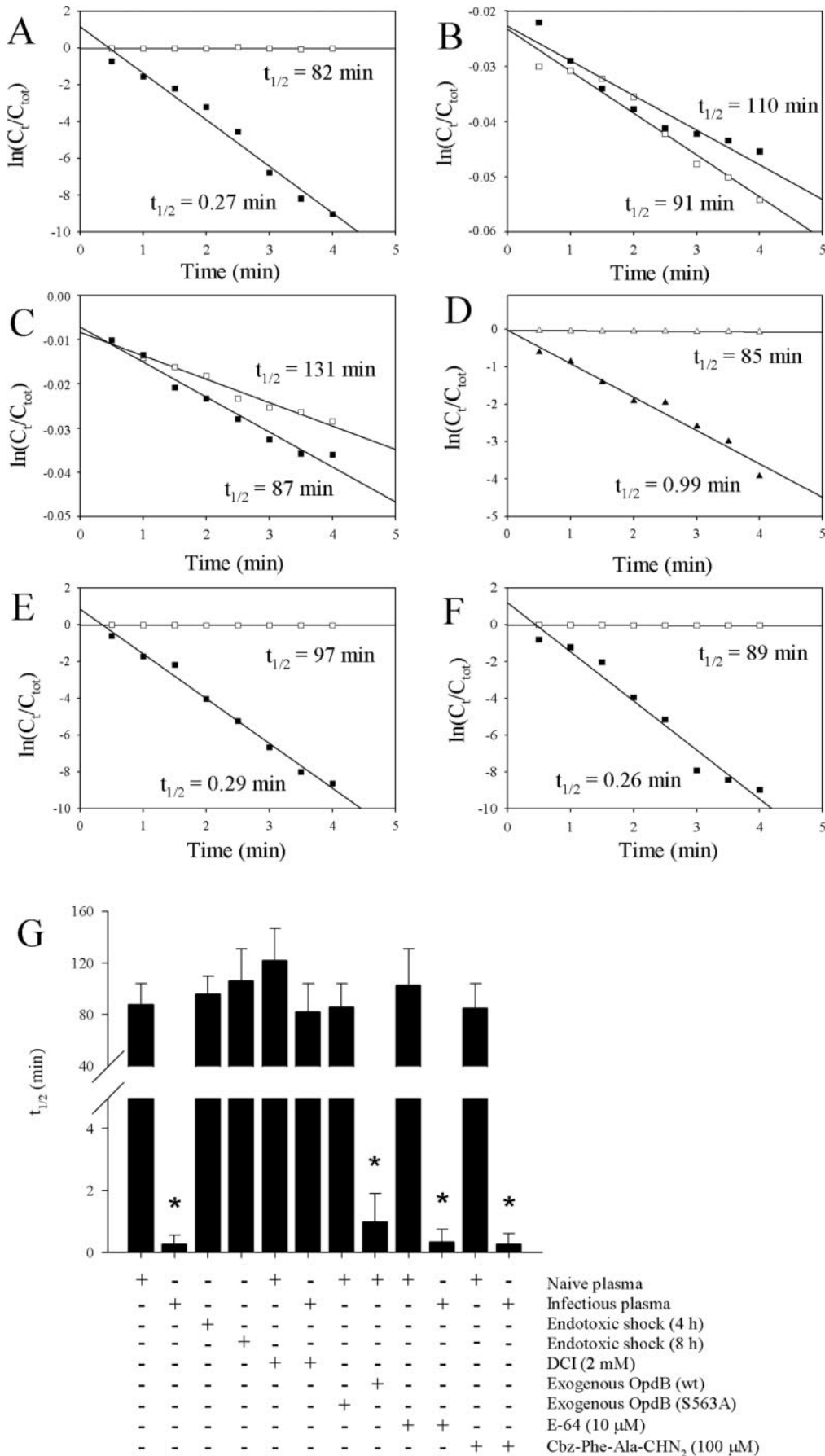
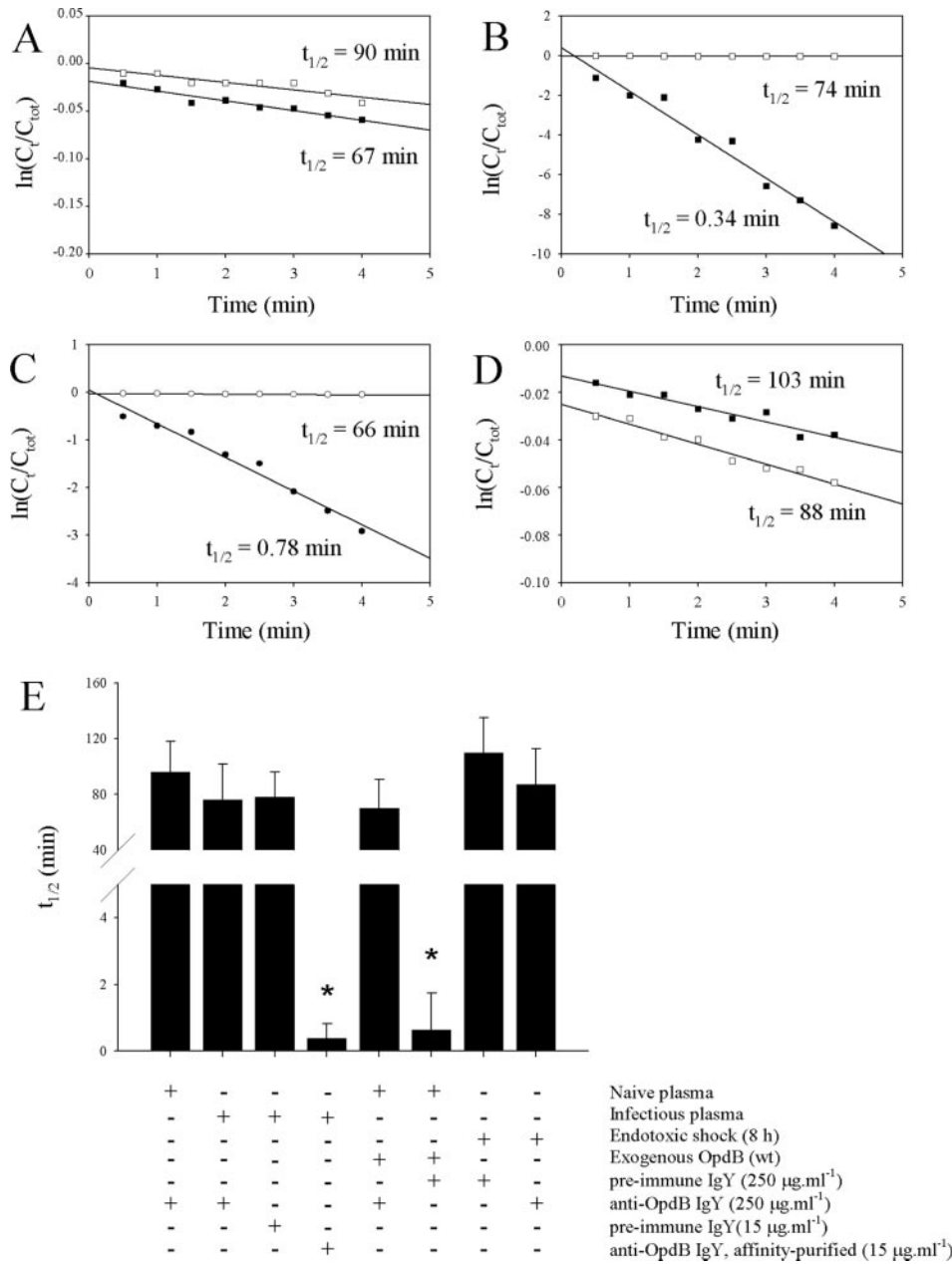


FIG. 7. Oligopeptidase B reduces the plasma half-life of <sup>125</sup>I-ANF. A, half-life of <sup>125</sup>I-ANF-(1-28) in cell- and parasite-free plasma extracted from healthy rats (□;  $r^2 = 0.87$ ) and in plasma extracted from *T. evansi*-infected rats (■;  $r^2 = 0.97$ ). B, half-life of <sup>125</sup>I-ANF-(1-28) in cell-free plasma extracted from rats challenged with LPS (20 mg·kg<sup>-1</sup>, intravenously) at 4 h (□;  $r^2 = 0.96$ ) and 8 h (■;  $r^2 = 0.91$ ) postchallenge. C, the effect of DCI



**FIG. 8. Anti-OpdB IgY abrogates  $^{125}\text{I}$ -ANF hydrolysis in plasma from *T. evansi*-infected rats.** A, the effect of 250  $\mu\text{g}\cdot\text{ml}^{-1}$  anti-OpdB IgY on the half-life of  $^{125}\text{I}$ -ANF-(1-28) in cell- and parasite-free plasma extracted from healthy rats ( $\square$ ;  $r^2 = 0.83$ ) and in plasma extracted from *T. evansi*-infected rats ( $\blacksquare$ ;  $r^2 = 0.93$ ). B, the effect of 15  $\mu\text{g}\cdot\text{ml}^{-1}$  affinity-purified anti-OpdB IgY ( $\square$ ;  $r^2 = 0.97$ ) and 15  $\mu\text{g}\cdot\text{ml}^{-1}$  preimmune IgY ( $\blacksquare$ ;  $r^2 = 0.99$ ) on the half-life of  $^{125}\text{I}$ -ANF-(1-28) in cell- and parasite-free plasma extracted from *T. evansi*-infected rats. C, effect of 250  $\mu\text{g}\cdot\text{ml}^{-1}$  preimmune IgY ( $\bullet$ ;  $r^2 = 0.96$ ) and 250  $\mu\text{g}\cdot\text{ml}^{-1}$  anti-OpdB IgY ( $\circ$ ;  $r^2 = 0.97$ ) on the half-life of  $^{125}\text{I}$ -ANF-(1-28) in healthy, cell-free plasma to which recombinant OpdB was exogenously added to a final activity of 2500  $\text{pmol}\cdot\text{s}^{-1}\cdot\text{ml}$  of plasma $^{-1}$ . D, effect of 250  $\mu\text{g}\cdot\text{ml}^{-1}$  preimmune IgY ( $\blacksquare$ ;  $r^2 = 0.92$ ) and 250  $\mu\text{g}\cdot\text{ml}^{-1}$  anti-OpdB IgY ( $\square$ ;  $r^2 = 0.93$ ) on the half-life of  $^{125}\text{I}$ -ANF-(1-28) in cell-free plasma from rats 8 h postchallenge with a lethal dose of LPS (20  $\text{mg}\cdot\text{kg}^{-1}$ ). A–D represent the raw data from a single, representative experiment. The averaged values of three independently determined half-lives for ANF *in vitro* for each experimental group are indicated in E for the experiments depicted in A–D. \*,  $p < 0.001$  compared with control values (the bar to the immediate left). Data reflect the mean ANF  $t_{1/2} \pm \text{S.D.}$  ( $n = 3$ ). wt, wild type.

tors in the vasculature. Considering that the  $t_{1/2}$  studies in live rats were performed at low to midlevel parasitemia (since animals with high parasitemia did not tolerate surgery) and

that plasma OpdB activity increases with increasing parasitemia (Fig. 2D), it is likely that the *in vivo*  $t_{1/2}$  of ANF in *T. evansi*-infected rats with high parasitemia would be even

(2 mM) on the half-life of  $^{125}\text{I}$ -ANF-(1-28) in cell- and parasite-free plasma extracted from healthy rats ( $\square$ ;  $r^2 = 0.98$ ) and in plasma extracted from *T. evansi*-infected rats ( $\blacksquare$ ;  $r^2 = 0.97$ ). D, effect of recombinant catalytically active OpdB ( $\blacktriangle$ ;  $\approx 1 \mu\text{g}\cdot\text{ml}^{-1}$  plasma; yielding a specific activity of 2500  $\text{pmol}\cdot\text{s}^{-1}\cdot\text{ml}$  of plasma $^{-1}$ ;  $r^2 = 0.97$ ) and recombinant, catalytically inactive OpdB(S563A) ( $\triangle$ ;  $\approx 1 \mu\text{g}\cdot\text{ml}^{-1}$  plasma;  $r^2 = 0.98$ ) on the half-life of  $^{125}\text{I}$ -ANF-(1-28) in healthy, cell-free plasma. E, the effect of E-64 (10  $\mu\text{M}$ ) on the half-life of  $^{125}\text{I}$ -ANF-(1-28) in cell- and parasite-free plasma extracted from healthy rats ( $\square$ ;  $r^2 = 0.96$ ) and in plasma extracted from *T. evansi*-infected rats ( $\blacksquare$ ;  $r^2 = 0.98$ ). F, the effect of Cbz-Phe-Ala-CHN<sub>2</sub> (100  $\mu\text{M}$ ) on the half-life of  $^{125}\text{I}$ -ANF-(1-28) in cell- and parasite-free plasma extracted from healthy rats ( $\square$ ;  $r^2 = 0.93$ ) and in plasma extracted from *T. evansi*-infected rats ( $\blacksquare$ ;  $r^2 = 0.96$ ). A–F represent the raw data from a single, representative experiment. The averaged values of three independently determined half-lives for ANF *in vitro* for each experimental group are indicated in G for the experiments depicted in A–F. \*,  $p < 0.001$  compared with control values (the bar to the immediate left). Data reflect the mean ANF  $t_{1/2} \pm \text{S.D.}$  ( $n = 3$ ). wt, wild type.

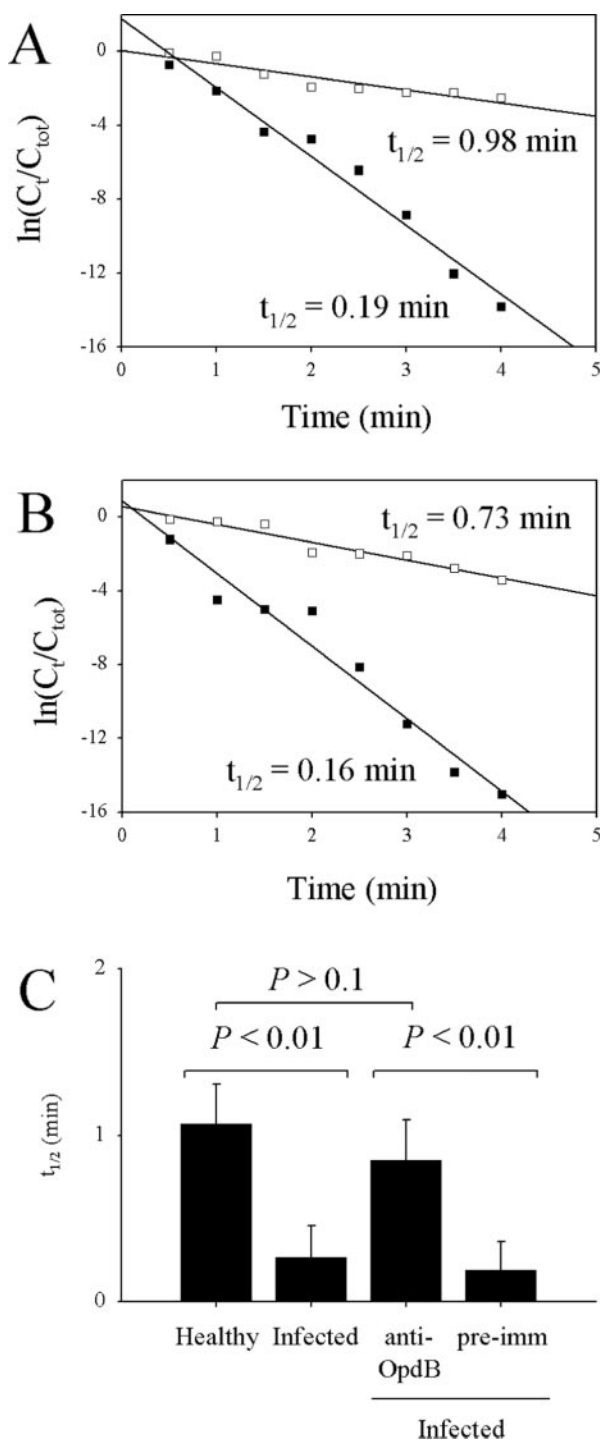


**FIG. 9. Oligopeptidase B reduces the *in vivo* plasma half-life of  $^{125}\text{I}$ -ANF.** A, plasma half-life of  $^{125}\text{I}$ -ANF-(1–28) *in vivo* injected into the jugular vein of healthy rats ( $\square$ ;  $r^2 = 0.87$ ) or *T. evansi*-infected rats at midlevel parasitemia ( $\blacksquare$ ;  $r^2 = 0.97$ ). B, plasma half-life of  $^{125}\text{I}$ -ANF-(1–28) *in vivo* injected into the jugular vein of *T. evansi*-infected rats at midlevel parasitemia that were preinfused for 2 h ( $20 \mu\text{g}\cdot\text{min}^{-1}$ ) with anti-OpdB IgY ( $\square$ ;  $r^2 = 0.93$ ) or preimmune IgY ( $\blacksquare$ ;  $r^2 = 0.92$ ). A and B represent the raw data from a single, representative experiment. The averaged values of three independently determined half-lives for ANF *in vitro* for each experimental group are indicated C for the experiments depicted in A and B. Data reflect the mean ANF  $t_{1/2} \pm$  S.D. ( $n = 3$ ). *pre-imm*, preimmune.

shorter. In further support of this idea, we infused anti-OpdB IgY into rats at midlevel parasitemia and determined the *in vivo* ANF  $t_{1/2}$ . The affinity-purified anti-OpdB IgY (or preimmune IgY) was infused to plasma concentrations above 100

$\mu\text{g}\cdot\text{ml}^{-1}$  of plasma $^{-1}$ , which is well in excess of what is required to block OpdB-mediated ANF hydrolysis *in vitro* in plasma from *T. evansi*-infected rats (Fig. 8, B and E). Infusion of the anti-OpdB IgY significantly elevated the ANF  $t_{1/2}$  to 0.78 min (Fig. 9, B and C), which compares well with the ANF  $t_{1/2}$  observed in healthy animals (1 min; Fig. 9, A and C). In contrast, infusion of preimmune IgY to  $100 \mu\text{g}\cdot\text{ml}^{-1}$  of plasma $^{-1}$  did not elevate the ANF  $t_{1/2}$  in *T. evansi*-infected rats but rather yielded a value (0.18 min) that is comparable with that obtained in *T. evansi*-infected rats that did not receive any infusion (Fig. 9, A and C). From these data, we conclude that peptidases released by *T. evansi* can modulate regulatory peptide hormone levels in the plasma of infected hosts. We further conclude that the bulk of ANF-degrading activity can be attributed to OpdB.

Given that  $k_{cat} = V_{max}/[E]_0$ , where  $V_{max}$  represents the maximum velocity and  $[E]_0$  represents the active enzyme concentration, we determined the  $V_{max}$  for Cbz-Arg-Arg-AMC hydrolysis using an aliquot of infected rat plasma under the same conditions that were used to determine the  $k_{cat}$  for purified OpdB. Normalizing for hydrolysis in the presence of anti-OpdB antibodies, we estimated the plasma OpdB concentration in infected rats at peak parasitemia at 16 nM. This is extremely high relative to the concentration of most bloodstream regulatory peptides such as ANF, which is present in the picomolar range. In our *in vitro* studies, we used 1:100 (mol:mol) OpdB:ANF ratios. In an infection, these ratios would be reversed. Given a normal plasma ANF concentration of  $\sim 125 \text{ pg}\cdot\text{ml}^{-1}$ , which translates to 42 pM, the OpdB:ANF (mol:mol) ratio in the plasma of infected animals is 400:1. The OpdB is in vast molar excess. Thus, we conclude that OpdB present in the bloodstream of infected animals, even at a low level of parasitemia, would yield sufficient OpdB activity in the plasma to modulate host peptide hormone levels. These data lend concrete support to the previously unproven idea that parasite peptidases released into the host circulation can modulate peptide hormone levels in the host plasma.

**A Role for OpdB-mediated ANF Degradation in Disease Pathogenesis**—The plasma levels of ANF are dramatically reduced in trypanosome infections in dogs (17) and in rats (this study). We have proposed in this study that OpdB is responsible for these reduced ANF levels. Could these reduced ANF levels contribute to the pathogenesis of trypanosomiasis? Elevated blood volume is a key characteristic of infection with bloodstream trypanosomes where blood volume increases up to 57% (21, 56). Blood volume is controlled by the atrium where baroreceptors respond to an increased blood volume load by secretion of ANF, which reduces blood volume through its vasorelaxant, hypotensive, diuretic, and natriuretic properties (57). In *T. brucei* infection in dogs, ANF granules are depleted in the atrial myocytes, the primary site of ANF synthesis and secretion (58), and the presence of distended Golgi complexes in the atria led Ndung'u *et al.* (17) to conclude that, during trypanosome infections, “synthesis of ANF is continuous and could not keep up with the rate of secretion.” Considering the findings that we report in this study, it may well be that the trypanosome-infected host is hypersecreting ANF in an effort to balance its rapid turnover in the plasma caused by trypanosome-derived OpdB. The host cannot sustain adequate ANF plasma levels, and infected animals are therefore unable to control the increased blood volume load (which more ANF would relieve). This elevated blood volume could lead to the many lesions observed in the circulatory system of trypanosome-infected hosts. These lesions include idiopathic cardiomyopathy, which is evident early in trypanosome infections (3, 46). Later there is extensive cardiac involvement including poor left ventricular function, valvular incompetence, atrioven-

tricular block, sinus arrest, and S-T segment elevation (59) and congestive heart failure (60), all of which may be caused by hypervolemia (increased blood volume load) (61), with death frequently resulting from heart failure (3). We propose here that the OpdB-mediated reduction in plasma ANF, with consequent loss of control of blood volume, contributes to the development of this pathology.

**Acknowledgments**—We thank Oliver Eickelberg for outstanding support, Luiz Juliano and Philippe Grellier for expert advice and for reading the manuscript, and Kevin H. Mayo for helpful comments.

## REFERENCES

- Hoare, C. A. (1972) *The Trypanosomes of Mammals*, Blackwell Scientific Publications, Oxford
- Brun, R., Hecker, H., and Lun, Z. R. (1998) *Vet. Parasitol.* **79**, 95–107
- Tizard, I., Nielsen, K. H., Seed, J. R., and Hall, J. E. (1978) *Microbiol. Rev.* **42**, 664–681
- Jaffe, C. L., and Dwyer, D. M. (2003) *Parasitol. Res.* **91**, 229–237
- Okenu, D. M., Opara, K. N., Nwuba, R. I., and Nwagwu, M. (1999) *Parasitol. Res.* **85**, 424–428
- Santana, J. M., Grellier, P., Schrevel, J., and Teixeira, A. R. (1997) *Biochem. J.* **325**, 129–137
- Morty, R. E., Lonsdale-Eccles, J. D., Mentele, R., Auerswald, E. A., and Coetzer, T. H. (2001) *Infect. Immun.* **69**, 2757–2761
- Del Nery, E., Juliano, M. A., Lima, A. P., Scharfstein, J., and Juliano, L. (1997) *J. Biol. Chem.* **272**, 25713–25718
- Heumann, D., Burger, D., Vischer, T., de Colmenares, M., Bouvier, J., and Bordier, C. (1989) *Mol. Biochem. Parasitol.* **33**, 67–72
- Troeberg, L., Pike, R. N., Morty, R. E., Berry, R. K., Coetzer, T. H., and Lonsdale-Eccles, J. D. (1996) *Eur. J. Biochem.* **238**, 728–736
- Lonsdale-Eccles, J. D., Mpimbaza, G. W., Nkhungulu, Z. R., Olobo, J., Smith, L., Tosomba, O. M., and Grab, D. J. (1995) *Biochem. J.* **305**, 549–556
- Morty, R. E., Lonsdale-Eccles, J. D., Morehead, J., Caler, E. V., Mentele, R., Auerswald, E. A., Coetzer, T. H., Andrews, N. W., and Burleigh, B. A. (1999) *J. Biol. Chem.* **274**, 26149–26156
- Morty, R. E., Authié, E., Troeberg, L., Lonsdale-Eccles, J. D., and Coetzer, T. H. (1999) *Mol. Biochem. Parasitol.* **102**, 145–155
- Burleigh, B. A., Caler, E. V., Webster, P., and Andrews, N. W. (1997) *J. Cell Biol.* **136**, 609–620
- Santana, J. M., Grellier, P., Rodier, M. H., Schrevel, J., and Teixeira, A. (1992) *Biochem. Biophys. Res. Commun.* **187**, 1466–1473
- Grellier, P., Vendeville, S., Joyeau, R., Bastos, I. M., Drobecq, H., Frappier, F., Teixeira, A. R., Schrevel, J., Davioud-Charvet, E., Sergheraert, C., and Santana, J. M. (2001) *J. Biol. Chem.* **276**, 47078–47086
- Ndung'u, J. M., Wright, N. G., Jennings, F. W., and Murray, M. (1992) *Parasitol. Res.* **78**, 553–556
- Tetaert, D., Soudan, B., Huet-Duvillier, G., Degand, P., and Boersma, A. (1993) *Int. J. Pept. Protein Res.* **41**, 147–152
- Soudan, B., Tetaert, D., Hublart, M., Racadot, A., Croix, D., and Boersma, A. (1993) *Exp. Clin. Endocrinol.* **101**, 166–172
- Boreham, P. F., and Wright, I. G. (1976) *Br. J. Pharmacol.* **58**, 137–139
- Anosa, V. O., and Isoun, T. T. (1976) *Trop. Anim. Health Prod.* **8**, 14–19
- Abebe, G., Eley, R. M., and ole-MoiYoi, O. K. (1993) *Acta Endocrinol. (Copenh.)* **129**, 75–80
- Hublart, M., Tetaert, D., Croix, D., Boutignon, F., Degand, P., and Boersma, A. (1990) *Acta Trop.* **47**, 177–184
- Desquesnes, M., and Tresse, L. (1996) *Rev. Elev. Med. Vet. Pays Trop.* **49**, 322–327
- Pellé, R., and Murphy, N. B. (1993) *Mol. Biochem. Parasitol.* **59**, 277–286
- Schagger, H., and von Jagow, G. (1987) *Anal. Biochem.* **166**, 368–379
- Aiyar, A. (2000) *Methods Mol. Biol.* **132**, 221–241
- Morty, R. E., Fülöp, V., and Andrews, N. W. (2002) *J. Bacteriol.* **184**, 3329–3337
- Hermanson, G. T., Mallia, A. K., and Smith, P. K. (1992) *Immobilized Affinity Ligand Techniques*, Academic Press, San Diego, CA
- Bradford, M. M. (1976) *Anal. Biochem.* **72**, 248–254
- Thibault, G., Lazure, C., Schiffrin, E. L., Gutkowska, J., Chartier, L., Garcia, R., Seidah, N. G., Chretien, M., Genest, J., and Cantin, M. (1985) *Biochem. Biophys. Res. Commun.* **130**, 981–986
- Hemerly, J. P., Oliveira, V., Del Nery, E., Morty, R. E., Andrews, N. W., Juliano, M. A., and Juliano, L. (2003) *Biochem. J.* **373**, 933–939
- Grab, D. J., Webster, P., Ito, S., Fish, W. R., Verjee, Y., and Lonsdale-Eccles, J. D. (1987) *J. Cell Biol.* **105**, 737–746
- Maugeri, D. A., and Cazzulo, J. J. (2004) *FEMS Microbiol. Lett.* **234**, 117–123
- Steiger, R. F., Oppendoes, F. R., and Bontemps, J. (1980) *Eur. J. Biochem.* **105**, 163–175
- Wise, W. C., Cook, J. A., Tempel, G. E., Reines, H. D., and Halushka, P. V. (1989) *Prog. Clin. Biol. Res.* **299**, 243–252
- Simonsen, U., Wadsworth, R. M., Buus, N. H., and Mulvany, M. J. (1999) *J. Physiol.* **516**, 271–282
- Schechter, I., and Berger, A. (1967) *Biochem. Biophys. Res. Commun.* **27**, 157–162
- Fülöp, V., Böcskei, Z., and Polgár, L. (1998) *Cell* **94**, 161–170
- Fülöp, V., Szeltnér, Z., and Polgár, L. (2000) *EMBO Rep.* **1**, 277–281
- Yamaguchi, K., Majima, M., Katori, M., Kakita, A., and Sugimoto, K. (2000) *Shock* **14**, 535–543
- Sugiyama, M., Fukumi, H., Grammer, R. T., Misono, K. S., Yabe, Y., Morisawa, Y., and Inagami, T. (1984) *Biochem. Biophys. Res. Commun.* **123**, 338–344
- Thibault, G., Garcia, R., Carrier, F., Seidah, N. G., Lazure, C., Chretien, M., Cantin, M., and Genest, J. (1984) *Biochem. Biophys. Res. Commun.* **125**, 938–946
- Misono, K. S., Grammer, R. T., Fukumi, H., and Inagami, T. (1984) *Biochem. Biophys. Res. Commun.* **123**, 444–451
- Olins, G. M., Spear, K. L., Siegel, N. R., and Zurcher-Neely, H. A. (1987) *Biochim. Biophys. Acta* **901**, 97–100
- Biswas, D., Choudhury, A., and Misra, K. K. (2001) *Exp. Parasitol.* **99**, 148–159
- Sugimoto, K., Shindo, M., Owada, T., Majima, M., and Katori, M. (1992) *Agents Actions Suppl.* **38**, 376–384
- Lubbesmeyer, H. J., Woodson, L., Traber, L. D., Flynn, J. T., Herndon, D. N., and Traber, D. L. (1988) *Am. J. Physiol.* **254**, R567–R571
- Rao, P. S., Cavanagh, D., Graham, D., Graham, L. B., Dietz, J. R., Fiorica, J. V., and Hoffman, M. S. (1998) *Am. J. Obstet. Gynecol.* **179**, 21–27
- Condra, C. L., Leidy, E. A., Bunting, P., Colton, C. D., Nutt, R. F., Rosenblatt, M., and Jacobs, J. W. (1988) *J. Clin. Invest.* **81**, 1348–1354
- Maack, T., Suzuki, M., Almeida, F. A., Nussenzweig, D., Scarborough, R. M., McEnroe, G. A., and Lewicki, J. A. (1987) *Science* **238**, 675–678
- Mackey, Z. B., O'Brien, T. C., Greenbaum, D. C., Blank, R. B., and McKerrow, J. H. (2004) *J. Biol. Chem.* **279**, 48276–48433
- Troeberg, L., Morty, R. E., Pike, R. N., Lonsdale-Eccles, J. D., Palmer, J. T., McKerrow, J. H., and Coetzer, T. H. (1999) *Exp. Parasitol.* **91**, 349–355
- Gros, C., Souque, A., and Schwartz, J. C. (1990) *Eur. J. Pharmacol.* **179**, 45–56
- Murthy, K. K., Thibault, G., and Cantin, M. (1988) *Biochem. J.* **250**, 665–670
- Goossens, B., Osaer, S., Kora, S., and Ndao, M. (1998) *Vet. Parasitol.* **79**, 283–297
- Maack, T. (1996) *Kidney Int.* **49**, 1732–1737
- de Bold, A. J. (1982) *Proc. Soc. Exp. Biol. Med.* **170**, 133–138
- Ndung'u, J. M. (1991) *J. Small Anim. Pract.* **32**, 579–584
- Morrison, W. I., Murray, M., Sayer, P. D., and Preston, J. M. (1981) *Am. J. Pathol.* **102**, 168–181
- Harris, P. (1987) *Br. Heart J.* **58**, 190–203